A Cable-Driven Exoskeleton With Personalized Assistance Improves the Gait Metrics of People in Subacute Stroke

Bin Zhong, *Student Member, IEEE*, Mei Shen, Haowen Liu, Yijun Zhao, Qiuyang Qian, Wei Wang, Haoyong Yu, *Senior Member, IEEE*, and Mingming Zhang, *Senior Member, IEEE*

***Abstract*— Most stroke survivors have mobility deficits and show a pathological gait pattern. Seeking to enhance the gait performance among this population, we have developed a hybrid cable-driven lower limb exoskeleton (called *SEAExo*). This study aimed to determine the effects of *SEAExo* with personalized assistance on immediate changes in gait performance of people after stroke. Gait metrics (i.e., the foot contact angle, knee flexion peak, temporal gait symmetry indices) and muscle activities were the primary outcomes to evaluate the assistive performance. Seven subacute stroke survivors participated and completed the experiment with three comparison sessions, i.e., walking without *SEAExo* (served as baseline) and without/with personalized assistance, at their preferred walking speeds. Compared to the baseline, we observed increases in the foot contact angle and knee flexion peak by 70.1% ($p < 0.05$) and 60.0% ($p < 0.05$) with personalized assistance. Personalized assistance contributed to the improvements in temporal gait symmetry of more impaired participants ($p < 0.05$), and it led to a 22.8% and 51.3% ($p < 0.05$) reduction in the muscle activities of ankle flexor muscles. These results demonstrate that *SEAExo* with personalized assistance has the potential to enhance post-stroke gait rehabilitation in real-world clinical settings.**

***Index Terms*— Assistance, exoskeleton, gait metric, gait symmetry, rehabilitation, stroke, walking.**

Manuscript received 1 November 2022; revised 5 February 2023, 4 April 2023, and 1 May 2023; accepted 26 May 2023. Date of publication 30 May 2023; date of current version 9 June 2023. This work was supported in part by the National Natural Science Foundation of China under Grant 62273173; in part by the Natural Science Foundation of Shenzhen under Grant JCYJ20210324104203010; in part by the Shenzhen Key Laboratory of Smart Healthcare Engineering under Grant ZDSYS20200811144003009; in part by the National Key Research and Development Program of China under Grant 2022YFF1202500 and Grant 2022YFF1202502; in part by the Guangdong Provincial Key Laboratory of Advanced Biomaterials under Grant 2022B1212010003; in part by the Research Program of Guangdong Province under Grant 2020ZDZX3001 and Grant 2019ZT08Y191; and in part by the Agency for Science, Technology and Research, Singapore, through the National Robotics Program, with A*STAR Science and Engineering Research Council (SERC) under Grant 1922500045. *(Bin Zhong, Mei Shen, and Haowen Liu contributed equally to this work.) (Corresponding authors: Haoyong Yu; Mingming Zhang.)*

This work involved human subjects or animals in its research. Approval of all ethical and experimental procedures and protocols was granted by the Medical Research Ethics Committee of the People's Hospital of Longhua under the Application No. LHPHMEC2022-085.

Bin Zhong is with the Shenzhen Key Laboratory of Smart Healthcare Engineering, Guangdong Provincial Key Laboratory of Advanced Biomaterials, Department of Biomedical Engineering, Southern University of Science and Technology, Shenzhen 518055, China, and also with the Department of Biomedical Engineering, National University of Singapore, Singapore 117583.

Mei Shen, Qiuyang Qian, and Wei Wang are with the Department of Rehabilitation Medicine, People's Hospital of Longhua, Shenzhen, Guangdong 518109, China.

Haowen Liu, Yijun Zhao, and Mingming Zhang are with the Shenzhen Key Laboratory of Smart Healthcare Engineering, Guangdong Provincial Key Laboratory of Advanced Biomaterials, Department of Biomedical Engineering, Southern University of Science and Technology, Shenzhen 518055, China (e-mail: zhangmm@sustech.edu.cn).

Haoyong Yu is with the Department of Biomedical Engineering, National University of Singapore, Singapore 117583 (e-mail: bieyhy@nus.edu.sg).

Digital Object Identifier 10.1109/TNSRE.2023.3281409

I. Introduction

STROKE is a leading cause of movement disability worldwide [1]. People with stroke usually exhibit pathological gait and balance disorders associated with joint deficits (e.g., foot drop and limited knee flexion motion) and adopt compensatory mechanisms (e.g., hip hiking and circumduction) during walking [2]. Correcting their gait patterns during gait training contributes to regaining independent mobility, which is regarded as a priority in post-stroke rehabilitation [3].

Post-stroke rehabilitation towards ambulatory function recovery follows the widely accepted principle that intensive and task-specific training is beneficial to improved outcomes [4]. Given this fact, various electric exoskeletons emerged in the past decades to enhance the effectiveness of the rehabilitation process and reduce the burden on physical therapists [5]. Meanwhile, numerous assistive strategies have been proposed and evaluated. The strategies towards gait rehabilitation usually include the position profile control [6], [7], torque profile control [8], [9], assist-as-needed strategy based on impedance control [10], [11], and proportional joint torque control [12], [13]. Another fact is that the pathological gait pattern is heterogeneous, and post-stroke survivors adapt differently to assistive intervention even in the same settings. Therefore, personalized assistive strategy to suit individual gait pattern has drawn a growing interest among researchers. Such strategies induced adjustable parameters for manual or automatic tuning of assistive torque profiles and proved their feasibility by achieving reduced metabolic cost [14], [15] or faster

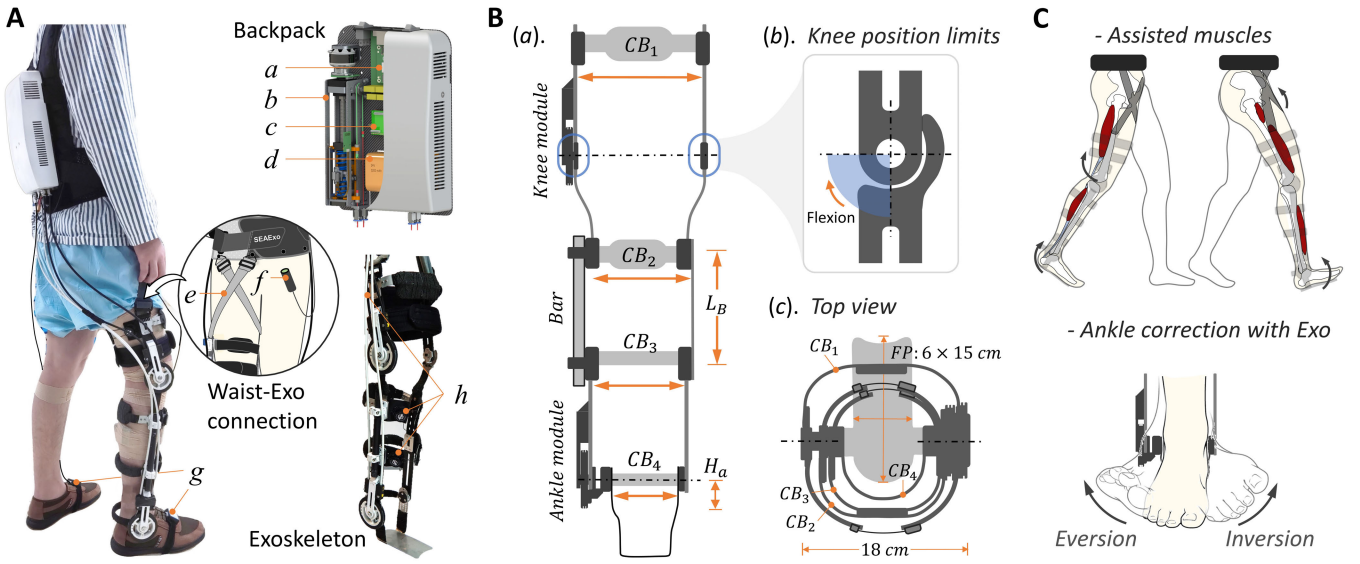

Fig. 1. **A.** Overview of the exoskeleton: *a*- control circuit (Raspberry CM4 & STM32F407 based circuit); *b*- series elastic actuator (SEA) connecting the inner cables; *c*- motor drivers (Elmo Gold Twitter); *d*- 24V battery; *e*- elastic bands; *f*- mode switch button (pressed to switch to Z.I.C mode); *g*- 9-axis IMU sensors; *h*- BOA lacing system. **B.** Configuration: (a). Envelope of the exoskeleton (orange arrows indicate the adjustable parts). (b). Mechanical limits on knee joints. (c). Top view of the exoskeleton in nominal size setting (foot plate size: 40-42 in EU scale). **C.** Assistance and physical correction for users' lower extremity. **Note*: the exoskeleton can be reassembled to be worn on the left side.

walking speed in healthy people [16] and improved spatial gait symmetry for people with chronic stroke [17]. Nevertheless, strategies with optimization-oriented tuning processes, such as human-in-the-loop optimization for maximum energy reduction, required a long exposure time and usually relied on a single optimization metric to assess assistive performance, hindering broader application in clinical settings.

In reality, it is challenging and time-consuming for investigators to determine the optimal assistance parameters based only on measured human performance. Besides, users expect not only a statistical outcome demonstrating the effectiveness of the device (e.g., users were unable to perceive a reduction in metabolic cost less than 22 $\pm$ 5.35% [18]), but also the comfort, safety, and acceptance during human-robot interaction based on our previous clinical questionnaire study [19]. Instead, incorporating user preference into the control of the exoskeleton (i.e., users determine the optimal assistance based on their own experiences and criteria) would significantly reduce the tuning burden and increase users' acceptance of the robotic device [20].

In addition, from a biomechanical perspective, human users benefit more from a robotic device when multi joints are appropriately assisted [21]. However, more powered robotic joints in wearable exoskeletons mean additional mass on the user's body and higher system complexity. Therefore, reported portable devices for post-stroke gait rehabilitation mainly focus on assisting single human joint, such as assist-on the hip joint [22], [23], ankle joint [7], [17], [24], [25], and knee joint [26], [27]. Devices with multi-active joints usually adopted entire rigid structures to transfer the system weight to the ground [2], leading to compromised wearability.

We have developed a hybrid cable-driven exoskeleton to assist the hip, knee and ankle joints of post-stroke users' paretic side while minimizing the worn mass. The "hybrid" concept is embodied in our design with passive assistance on the hip joint and active assistance on the knee and ankle joints. Antagonistically arranged elastic bands provide passive assistance, and two series elastic actuators (SEA) generate active assistance. This device is worn unilaterally on the paretic limb. This study aimed to investigate the immediate effects of personalized robotic assistance from *SEAExo* considering post-stroke users' preference on users' gait performance, which is less discussed in the wearable exoskeleton domain. To meet our study goal, we established a torque profile function with parameters for tuning the robotic assistance's amplitude, peak timing, and slopes to personalize individual assistance. The personalized assistance is time-adapted based on individual gait characteristics (i.e., gait cycle duration, timings of toe-off and initial foot contact) of previous strides and the current walking state. Then, we carried out three comparison sessions and evaluated participants' walking performance via biomechanical outcomes, i.e., gait metrics, changes in muscle activities, and foot pitch symmetry. The results will underpin the feasibility of *SEAExo* in clinical application.

II. Materials and Methods

A. Apparatus Description

This device (see **Fig. 1A**) was updated based on our previous system [28] with new design and features: 1) Two resistance exercise bands are leveraged to store and release mechanical energy throughout a gait cycle. They are arranged antagonistically on the anterior thigh connecting the exoskeleton and waist belt with pretension. The bands are configured in this setting based on the fact that stroke survivors exhibit weakness and fatigue of the hip flexors during walking, leading to compensatory hip hiking [29]; 2) an insole foot structure allows the exoskeleton to be worn with users' regular shoes.

This device benefits from the cable-driven transmission, introducing a low inertia burden on the user's paretic leg. 71.1% (3.2 kg) of the system's mass is loaded over the user's waist. The exoskeleton can work in two modes: 1) the force tracking control (F.T.C) mode providing desired assistance,

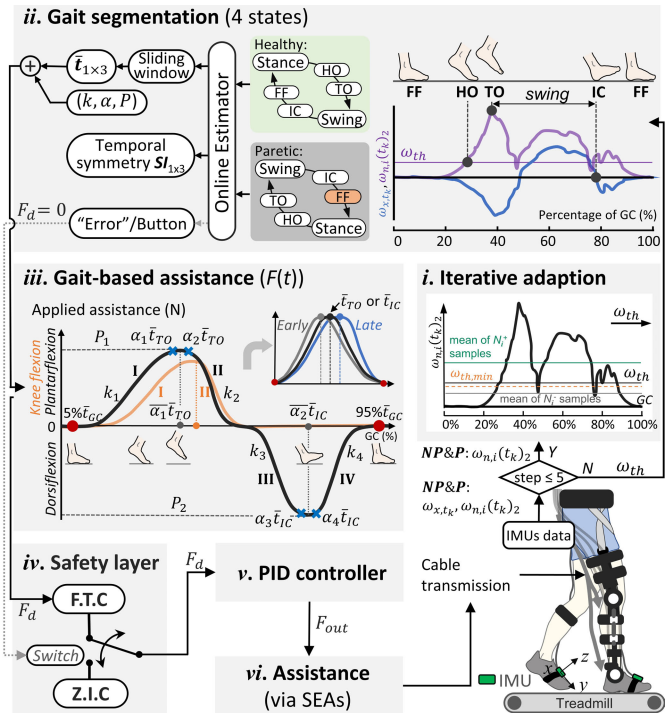

Fig. 2. Control loop of *SEAExo*. Data from two instep-mounted IMUs (P: paretic, NP: non-paretic) were utilized. After the iterative threshold adaption, an online estimator was designed for segmenting the gait, evaluating the gait characteristics, and error detection. Obtained toe-off timing t_{TO}, initial contact timing t_{IC}, and the gait duration t_{GC} were averaged via a sliding window. Considering the averaged timings $\bar{t}_{1\times3}$, $\bar{t}_{TO}$ and $\bar{t}_{IC}$ were key timings to shape the assistance (F_d). 5%$\bar{t}_{GC}$ and 95%$\bar{t}_{GC}$ were the start and end of the assistance. Safety layer had also been integrated, and a PID controller was used for force control.

and 2) the zero impedance control (Z.I.C) mode enabling the user to walk freely with the exoskeleton. Participants can use a handheld button to immediately switch the working mode of the exoskeleton from F.T.C to Z.I.C if they perceive discomfort, fatigue, or inappropriate gait during the experiments. The adopted linear series elastic actuator (see **Fig. 1A**), consisting of a brushless motor, a ball screw, and two springs (stiffness: 46 N·mm^{-1}), guarantees compliant user-robot interaction and is able to provide a peak torque of 17 N·m.

As shown in **Fig. 1B**, the exoskeleton consists of two main parts: the thigh-shank and the shank-ankle structures, which are connected by a carbon fiber bar. The exoskeleton is adjustable to accommodate a wide range of limb sizes by assembling different sizes of connecting bars (CB_1 to CB_4). Three optional sizes (i.e., 36-39, 40-42, and 43-45 in EU scale) of the foot plate (FP) are available and interchangeable. Each FP has an adjustable height (H_a) range of 5 cm with a series of 3 mm bolt holes. In the sagittal plane, the exoskeleton allows a range of motion of [0, 90°] and [−40°, 40°] for the knee and ankle joints, respectively. The radius of robotic joints is 35 mm. Position limits were set on the knee joint to avoid hyperextension of the knee. Moreover, the exoskeleton is low-profile and can be worn on either side of the lower limb by reassembling the connections. **Fig. 1C** illustrates the assisted muscles during walking and the physical correction of the ankle inversion/eversion deficit with a rigid frame.

An off-board microcontroller (STM32F407) takes desired torque command as input to control two SEAs at 500 Hz (see **Fig. 1A**). An upper controller (Raspberry CM4) utilizes the sensor data to perform online gait segmentation and gait metric estimation at 100 Hz, and all the data will be stored.

B. Gait Segmentation/Characteristics and Safety Layer

1) Gait Segmentation Method: To detect the user's real-time walking status, an online gait estimator (see **Fig. 2 *ii***) was established based on the angular velocity of the instep-mounted IMUs to segment a full gait cycle (GC) by four subsequent events, i.e., the foot flat (FF), heel off (HO), toe off (TO), and initial contact (IC). The segmentation followed a rule-based algorithm: 1) FF: the norm value of angular velocity ω_n ($\omega_n = (\omega_x^2 + \omega_y^2 + \omega_z^2)^{\frac{1}{2}}$) remains under a threshold ω_{th} for at least ten samples; 2) HO: one sample of ω_n exceeds the ω_{th} after FF; 3) TO: indicated by the peak of ω_n after HO when $\omega_x < 0$; 4) IC: indicated by the zero-velocity-crossing sequence of sagittal angular velocity ω_x after TO. FF is the start of each step, and FF on paretic side triggers the assistance.

2) Iterative Threshold Adaption: In clinical settings, walking speeds vary among post-stroke participants. The threshold ω_{th} has to be adapted based on gait velocity and sensor characteristics (i.e., angular velocity) to guarantee an accurate detection of FF and HO of both sides across individuals. Hence, we have implemented an iterative threshold adaption (see **Fig. 2 *i***) to automatically adjust the gait segmentation threshold ω_{th} for different individuals, as equations (1) to (4):

$$\omega_{\mathrm{th},1} := \frac{1}{2}\left(\max_{t_k\in[t_1,t_N]} \omega_{n,0}\,(t_k) + \min_{t_k\in[t_1,t_N]} \omega_{n,0}\,(t_k)\right) \quad (1)$$

$$N_i^+ := \left\{t_k \in [t_1, t_N] \mid \omega_{n,i}\,(t_k) > \omega_{\mathrm{th},i}\right\} \quad (2)$$

$$N_i^- := \left\{t_k \in [t_1, t_N] \mid \omega_{n,i}\,(t_k) \le \omega_{\mathrm{th},i}\right\} \quad (3)$$

$$\omega_{\mathrm{th},i+1} := \frac{W^-}{N_i^-}\sum_{t_k\in N_i^-} \omega_{n,i}\,(t_k) + \frac{W^+}{N_i^+}\sum_{t_k\in N_i^+} \omega_{n,i}\,(t_k) \quad (4)$$

where the start timing t_1 and end timing t_N of the current step $step_i$ are the adjacent foot flat timings $(t_{FF,i}, t_{FF,i+1})$ of $step_i$ and the next step $step_{i+1}$. t_k denotes the sampling time, $t_k \in [t_{FF,i}, t_{FF,i+1}]$. $\omega_{\mathrm{n},i}(t_k)$ is the ω_n values in $step_i$. The initial threshold $\omega_{th,1}$ is the mean value of the detected maximum and minimum $\omega_{n,0}(t_k)$ at the start step $step_0$, and $\omega_{th,i+1}$ is the threshold for the next step. N_i^+ and N_i^- are the counts of the samples that $\omega_{n,i}(t_k)$ is larger and smaller than the threshold value $\omega_{th,i}$, respectively, and the corresponding weighting parameters ($W^+ = 0.1$, $W^- = 0.9$) were preset. A lower bound ($\omega_{th,min} = 0.61$ rad·s^{-1}) was also set (if the converged $\omega_{\mathrm{th},i+1} < \omega_{th,min}$, then $\omega_{\mathrm{th},i+1} = \omega_{th,min}$). The iterative threshold adaption was performed at the initial five steps ($step_1$ to $step_5$) to generate individual thresholds, and the device worked in Z.I.C mode during the adaptive process.

3) Gait Characteristics: At the beginning of each step ($step_i > 8$), the online estimator calculated an averaged timing matrix $\bar{\boldsymbol{t}}_{1\times3}$: ($\bar{t}_{TO}$, $\bar{t}_{IC}$, $\bar{t}_{GC}$) of previous three strides from the non-paretic side via a sliding window. These timings were used for constructing the desired assistance profile (F_d) for the current step. The online estimator also evaluated the

temporal symmetry indices $\boldsymbol{SI}_{1\times3}$: (SI, SI_{st}, SI_{sw}), including the overall temporal gait symmetry (SI) and the stance/swing duration symmetry (SI_{st}, SI_{sw}). $\boldsymbol{SI}_{1\times3}$ was defined as below (P: paretic, NP: non-paretic, ST: stance, SW: swing):

$$SI = \frac{P_{\mathrm{SW}}/P_{\mathrm{ST}}}{NP_{\mathrm{SW}}/NP_{\mathrm{ST}}}, SI_{st} = \frac{P_{\mathrm{ST}}}{NP_{\mathrm{ST}}}, SI_{sw} = \frac{P_{\mathrm{SW}}}{NP_{\mathrm{SW}}}. \quad (5)$$

4) Safety Layer: Considering users' safety and experience, an "Error" sign was also induced within the control loop in case of unexpected events during experiments, i.e., stop walking (translated into the counts of FF events of $step_i$ was greater than the total counts of $step_{i-1}$, i.e., $N_{FF,i} > N_{step,i-1}$) and extreme asymmetry ($SI \notin [0.4, 3.5]$). An "Error" sign would result in an immediate switch to Z.I.C mode (see **Fig. 2 *iv***).

C. Personalized Wearable Assistance

With the obtained individual gait characteristics, a time-based force controller generated desired assistance (F_d) as the input of a low-level PID controller (see **Fig. 2 *v***). The force controller shaped assistance profiles $F(t)$ for users' knee and ankle joints through piecewise *Sigmoid* functions, as equations (6) and (7):

Force curves I&II:

$$P_1 \cdot \left(\frac{1}{1+e^{k_1(\alpha_1 \cdot \bar{t}_{TO} - t)}} + \frac{1}{1+e^{k_2(t-\alpha_2 \cdot \bar{t}_{TO})}} \right) - P_1 \quad (6)$$

Force curves III&IV:

$$P_2 \cdot \left(\frac{-1}{1+e^{k_3(\alpha_3 \cdot \bar{t}_{IC} - t)}} + \frac{-1}{1+e^{k_4(t-\alpha_4 \cdot \bar{t}_{IC})}} \right) + P_2 \quad (7)$$

Each *Sigmoid* function contained three shaping parameters: the rising/falling slope k_i, the peak timing ratio α_i $(i \in 1, 2, 3, 4)$, and force amplitudes P_i $(i \in 1, 2)$. The amplitude of assistance was limited to under 25% body weight (BW) in this study. Tuning the parameters (k_i, α_i, P_i) enabled *SEAExo* to provide adjustable assistance, better accommodating users' gaits and preferences. Specifically, a knee flexion assistance profile $F(t)_{knee}$, consisting of force curves I&II, was applied at the user's knee joint and individually determined by five parameters $(k_1, k_2, \alpha_1, \alpha_2, P_1)$. An ankle assistance profile $F(t)_{ankle}$, consisting of force curves I-IV, was applied at the user's ankle joint and individually determined by ten parameters $(k_1, k_2, \alpha_1, \alpha_2, P_1, k_3, k_4, \alpha_3, \alpha_4, P_2)$.

The peak timings of flexion and extension assistance were defined as $\overline{\alpha_1} \cdot \bar{t}_{TO}$ and $\overline{\alpha_2} \cdot \bar{t}_{IC}$ $(\overline{\alpha_1} = 0.5 \cdot (\alpha_1 + \alpha_2), \overline{\alpha_2} = 0.5 \cdot (\alpha_3 + \alpha_4))$, respectively. Accordingly, we defined three types of profiles as follows (illustrated in subfigure of **Fig. 2 *iii***): 1) "*General*": a profile peaks at exact TO or IC timings $(\overline{\alpha_i} = 100\%$, illustrated as the black curve); 2) "*Early*": a profile with earlier peak timing $(\overline{\alpha_i} \in [60, 100)\%$, illustrated as the gray curve); 3) "*Late*": a profile with later peak timing $(\overline{\alpha_i} \in (100, 130]\%$, illustrated as the blue curve), $i \in 1, 2$.

D. Participants Recruitment

Participants were recruited from the Department of Rehabilitation Medicine, People's Hospital of Longhua, Shenzhen, China. Participants' eligibility requirements were as follows:

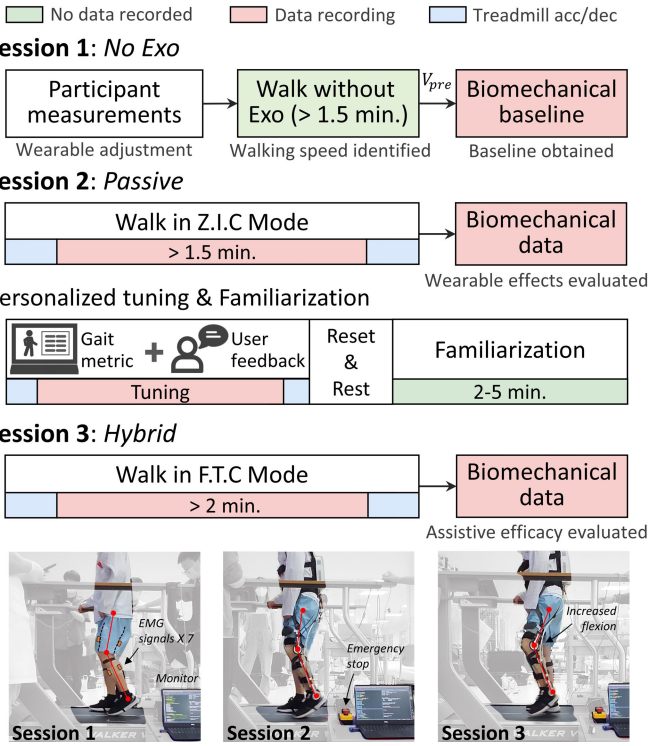

Fig. 3. Illustration of experimental protocol. Biomechanical data, including the gait metric, foot pitch, and surface electromyography (EMG) data from seven paretic leg muscles (i.e., vastus lateralis: VL, rectus femoris: RF, vastus medialis: VM, tibialis anterior: TA, lateral gastrocnemius: LG, medial gastrocnemius: MG, hamstrings: HM), were collected.

1) hemiplegic stroke $\leq$ six months, 2) height between 1.5 m and 1.85 m, 3) weight $<$ 80 kg, 4) cognition to follow experimental instructions and understand the content of study, 5) no excessive spasticity in the hip, 6) ability to walk independently for at least two minutes (min.), and 7) physician approval. Exclusion criteria included: 1) muscular injuries, 2) uncontrolled hypertension, 3) participation in another clinical trial, and 4) current deep vein thrombosis (DVT). This study was approved by the Medical Research Ethics Committee of the People's Hospital of Longhua under the approval number: LHPHMEC2022-085.

E. Experimental Protocol

A one-day experimental protocol with three treadmill-based sessions has been designed (see **Fig. 3**). Participants walked in their regular shoes. Each session was conducted thrice with a minimum of three min. of rest between trials.

First, we performed a session in which participants walked freely without the exoskeleton (referred to as the "*No Exo*" session). In this session, we identified the participants' limb sizes to customize the exoskeleton structure to achieve better human-robot alignment. Then, participants walked at their preferred speeds V_{pre}, which would be adopted throughout their experiments. The biomechanical data of 1.5 min. of walking were collected as the baseline.

Second, a wearable effects evaluation session was carried out (referred to as the "*Passive*" session). In this session, participants walked with the exoskeleton working in Z.I.C mode and passive assistance for hip flexion. We recorded at least 1.5 min. of the biomechanical data and compared the

TABLE I
IDENTIFICATION OF PARTICIPANTS' CHARACTERISTICS

Participant I.D.	Gender	Age (yrs)	Height (m)	Weight (kg)	Paretic side	Chronicity (mos)	Impairments	Brunnstrom	Daily walking aids	Speed (km/h)
P1	Male	40	1.66	53	Right	5	*abc*	III	Quadcane	1.0
P2	Male	37	1.64	65	Right	2	*abc*	III	AFO	1.0
P3	Female	35	1.50	49	Right	3	*abc*	III	AFO	1.2
P4	Male	56	1.60	62	Left	1	*abc*	IV	None	1.2
P5	Male	34	1.78	75	Left	5	$(c)^{\dagger}$	V	None	2.6
P6	Male	46	1.73	79	Left	6	*ac*	IV	None	1.0
P7	Male	20	1.75	64	Left	1.5	$(ac)^{\dagger}$	IV	None	2.4

Note: Impairments description: *a*: decreased knee flexion, *b*: knee hyperextension, *c*: foot drop. AFO: ankle foot orthosis. †: moderate gait impairments.

results to the baseline to evaluate the effects of walking with the exoskeleton and without assistance.

Before the final validation session, a parameter tuning process was designed for each participant, followed by a 2-5 min. of familiarization (see **Fig. 3**). During the tuning process, participants were instructed to walk with the initial assistance in the *General* setting (i.e., F_{knee}: $(10, 50, 100\%, 50N)$, F_{ankle}: $(15, 50, 100\%, 50N, 50, 50, 100\%, 50N)$). We first identified whether the proper peak timings of assistance were in the *General*, *Early*, or *Late* setting, according to the user's perception of the assistance (i.e., comfort, safety, mitigation of impairments, and reduced efforts in joint movements). The tuning interval for peak timing $\delta\overline{\alpha_i}$ was 10%. After that, we tuned the peak magnitude with a force interval of 30 N to roughly determine the upper bound of the assistance according to the user's perception. Then, we tuned the peak magnitude by 10 N to determine a proper amplitude P_i. The k_i values were also fine-tuned accordingly in these two procedures. The users' feedback helped reduce the tuning time, preventing us from testing a wide range of assistance profiles. Moreover, the gait symmetry index (*SI*) was also monitored throughout the tuning process. The preferred assistance was the one that achieved user preference while contributing to improved gait metrics compared to baselines (i.e., *SI* value tended to 1).

Finally, we conducted the validation session to investigate the overall effectiveness of the personalized assistance along with the passive hip flexion assistance on the user's gait improvements (referred to as the "*Hybrid*" session). We collected biomechanical data over two min. to evaluate the effects of personalized assistance.

F. Data Collection and Statistical Analysis

1) Kinematic Data: The kinematic data, i.e., the rotational angle, velocity, and orientation of two feet, and rotational angle of the paretic ankle and knee joints, were obtained from two instep-mounted IMUs (WT901C485, WitMotion, China) and encoders embedded in the SEAs [28].

2) Electromyographic Data: Muscle activities were recorded at 1000 Hz with seven EMG sensors (DataLITE, Biometrics Ltd., UK). Raw EMG data were offline processed through following steps: digitized the analog data; band-pass filtered (4^{th} order Butterworth, 10-250 Hz cut-off for removing noise); rectified by getting the absolute value; low-pass filtered (4^{th} order Butterworth, 4 Hz cut-off); normalized to mean peak value of the baseline condition; then, normalized values of each gait cycle were averaged to obtain the Mean Averaged Values (MAV) to quantify the muscle activities of each step.

3) Usability Rating: After the experiment, the participants were asked to rate the usability of *SEAExo* on a scale of 0 to 10 points. Specifically, [0 - 6.0]: Unsatisfied, (6.0 - 7.5]: Moderate, (7.5 - 9.0]: Satisfied, (9.0 - 10]: Excellent.

4) Statistical Analysis: Gait metrics and muscle activities were the primary outcomes of interest. We selected the gait metrics data of three min. for each session (one minute per trial) and the EMG data of 90 steps for each session (i.e., 30 steps per trial) to construct the raw data sets. The normality of raw data sets were rejected by Kolmogorov-Smirnov tests. Then, median values were further selected to construct the data sets for statistical analysis, and we used the Shapiro-Wilk tests to check the data normality. Differences in outcomes among the *No Exo*, *Passive*, and *Hybrid* sessions were evaluated as follows: a) For the normally distributed data, we used the one-way repeated ANOVA; b) For the non-normally distributed data (i.e., EMG data of the VM and MG muscles), we adopted Friedman's omnibus tests. Post-hoc Bonferroni and Dunn's tests were then conducted to evaluate the differences between each paired session, respectively. Specially, we used the paired-sample t-test for the statistical analysis of the changes in knee flexion peak (*Hybrid* v.s *Passive*). $p < 0.05$ indicates significance. All statistics were performed in OriginPro 2021b.

III. RESULTS

Seven participants (6 males; average age 38.3 ± 11.1 years, height 1.67 ± 0.09 m, weight 63.9 ± 10.8 kg) participated in this clinical study, and their characteristics have been listed in **Table I**. Prior to participation, all participants were presented with a clear explanation of the experimental contents and possible consequences of the study and provided written informed consent. Experiments were conducted in the presence of two physiotherapists, and participants completed all the sessions without walking aids (i.e., quadcane and AFO).

A. Personalized Assistance Parameters

Personalized assistance profiles labeled with the peak timing type (see **Fig. 4A&B**) and the distribution of peak timings of assistance profiles (see **Fig. 4C**) are presented. The profiles were normalized to the gait cycle starting from the IC event, and the specific individual assistance parameters are listed in **Table II**. For ankle plantarflexion (*PF*) assistance, the amplitude ranged from 4.9-20.8 %BW, and peaked at timing 70.7[60.0, 85.0]% of the TO. For ankle dorsiflexion (*DF*) assistance, the amplitude ranged from 11.5-20.8 %BW, and

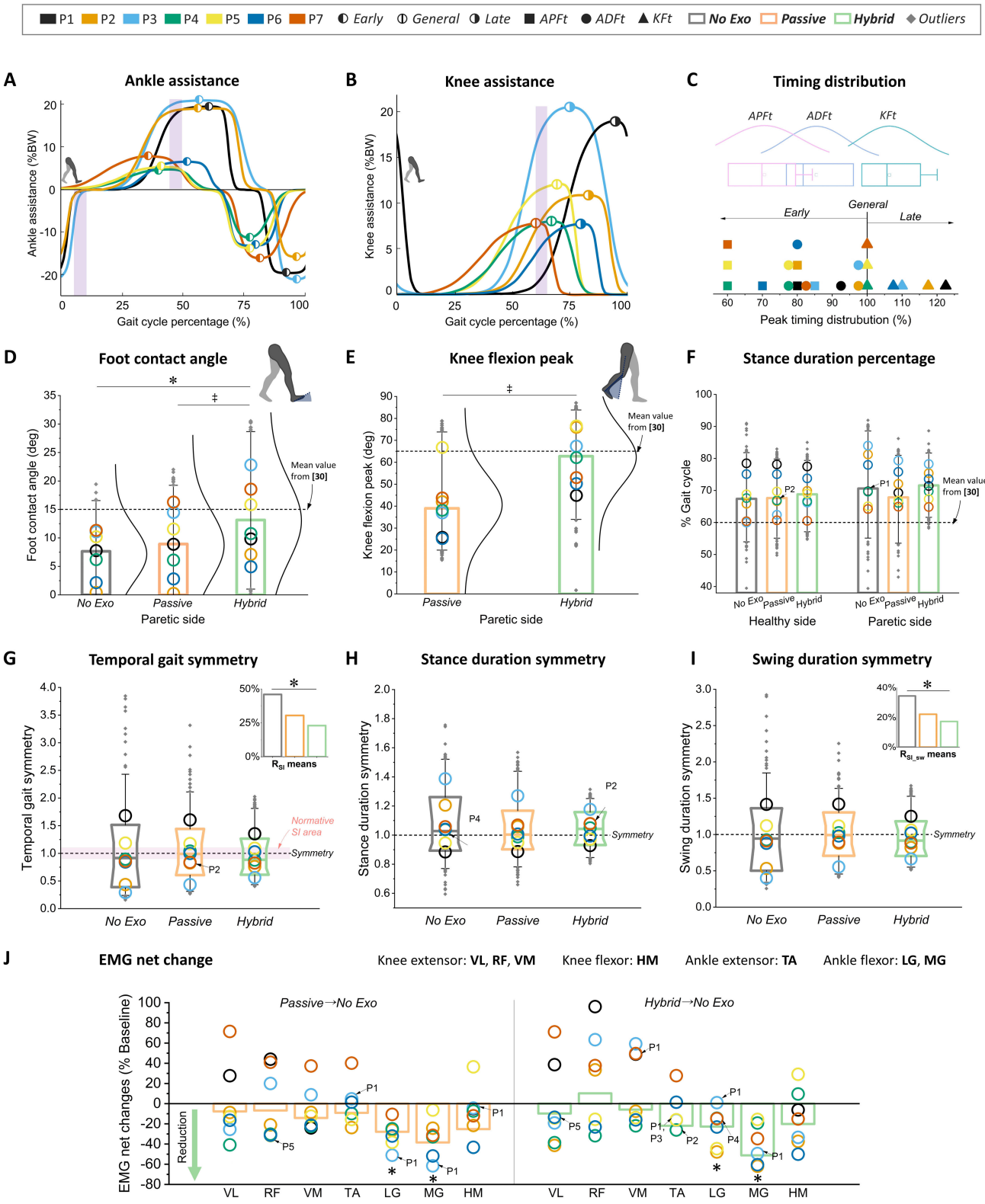

Fig. 4. Personalized assistance profiles and biomechanical results. **A**&**B**: Knee and ankle assistance profiles of participants. The transparent purple bars denote the ranges of peaks of ankle dorsiflexion, ankle plantarflexion, and knee flexion assistance (from left to right). **C**: Distribution of assistance peak timings (*APFt*: ankle plantarflexion assistance peak timings (%$\bar{t}_{TO}$), *ADFt*: ankle dorsiflexion assistance peak timings (%), *KFt*: knee flexion assistance peak timings (%$\bar{t}_{TO}$)). **D**-**J**: Biomechnical results in the group level and participant level (colored circles) in three experimental sessions (i.e., *No Exo*, *Passive*, and *Hybrid*). Results reported in medians and whiskers. **D**-**F**: Dash lines denote the average foot contact angle, knee flexion peak, and stance percentage of full gait cycle retrieved from healthy people [30]. Notably, the knee joint angle was measured via the sensors integrated in the exoskeleton, hence the flexion peak data in *No Exo* session was not collected and presented. **G**-**I**: Dash lines denote a temporal symmetry (i.e., symmetry index equals to one). Subplots are the mean values of the asymmetry ratio of temporal symmetry indices from five participants excluding P4 and P7. **J**: Changes in muscular activities of all participants relative to baseline. For this result, we care more about the difference between *Passive*/*Hybrid* session and the baseline. The overlapped individual data are indicated by arrows with labels. * and ‡: significance ($p<0.05$) relative to the *No Exo* and *Passive* session, respectively. Statistical outliers: values larger than 1.5x the IQR.

TABLE II
ASSISTANCE PARAMETERS AND USABILITY

I.D.	Parameters of $F(t): k_i(k_{rise}, k_{fall}), \alpha_i(\alpha_{rise}, \alpha_{fall}), P_i$		
	F_{PF}	F_{DF}	F_{KF}
P1	(15,55),(75,85),19.3	(50,50),(90,95),19.3	(10,35),(120,125),19.3
P2	(15,45),(75,85),18.8	(50,50),(95,100),15.7	(11,35),(115,120),11
P3	(15,25),(80,90),20.8	(50,40),(95,100),20.8	(10,35),(110,115),20.8
P4	(15,40),(60,60),4.9	(50,35),(75,80),11.5	(15,50),(95,105),8.2
P5	(15,45),(60,60),5.4	(50,35),(75,80),13.6	(12,58),(95,105),12.3
P6	(15,40),(65,75),6.5	(50,35),(75,85),12.9	(11,58),(105,110),7.8
P7	(15,40),(60,60),8	(50,35),(80,85),16	(11,60),(95,105),8
Individual usability rating (P1-P7): $(8.5, 8.0, 9.0, 8.0, 7.5, 8.0, 7.5)$			

peaked at timing 86.4[77.5, 97.5]% of the IC. For knee flexion (*KF*) assistance, the amplitude ranged from 7.8-20.8 %BW, and peaked at timing 108.2[100.0, 122.5]% of the TO. It can be seen that participants preferred the *KF* assistance applied in the *General* or *Late* settings, and the *PF* and *DF* assistance were consistently preferred in the *Early* settings when peak timings were determined by gait events TO and IC.

B. Effects on Gait Metrics

Bar (median) and box (10^{th} to 90^{th} percentile with median line) plots with the whiskers (1^{st} to 99^{th} percentile) for gait metrics results of interest are presented in this section.

As shown in **Fig. 4D&E**, the *SEAExo* increased participants' foot contact angle at heel strike ($F(2,5) = 9.55$, $p < 0.05$) and the knee flexion peak during swing phase ($t(6) = -6.01$, $p < 0.05$). In the *No Exo* and *Passive* sessions, participants walked with a median foot contact angle of 7.7 $\pm$ 3.9° (median $\pm$ sIQR) and 8.9 $\pm$ 5.4°, respectively. With the personalized assistance (i.e., in *Hybrid* condition), both statistical improvements were observed compared to the *No Exo* ($t(12) = 5.79$, $p < 0.05$) and *Passive* ($t(12) = 4.18$, $p < 0.05$) sessions, and foot contact angle increased to a median of 13.1 $\pm$ 5.7°. The participants also exhibited a significantly higher median knee flexion peak of 62.8 $\pm$ 11.3° ($p < 0.05$) in *Hybrid* session compared to the *Passive* session (39.0 $\pm$ 7.9°).

Seeing **Fig. 4F**, *SEAExo* did not induce statistical difference and obvious changes in participants' stance phase duration on both sides. Specifically, group-level changes in stance duration were less than 3% between *Passive* and *Hybrid* sessions and *No Exo* session.

In the group level, *SEAExo* did not show statistical influence on participants' temporal gait symmetry, stance duration symmetry, and swing duration symmetry (see **Fig. 4G-I**). Without the *SEAExo*, participants walked with temporal symmetry indices (SI, SI_{st}, SI_{sw}) of (0.91 $\pm$ 0.22, 1.03 $\pm$ 0.07, 0.94 $\pm$ 0.15). In the *Passive* session, participants' temporal symmetry indices changed to (0.99 $\pm$ 0.19, 1.00 $\pm$ 0.06, 0.99 $\pm$ 0.13). In the *Hybrid* session, participants presented median temporal symmetry indices of (0.88 $\pm$ 0.17, 1.04 $\pm$ 0.06, 0.92 $\pm$ 0.12). Nevertheless, those data appeared to be more tightly clustered around a symmetric gait pattern (i.e., $\boldsymbol{SI}_{1\times3} = (1, 1, 1)$) with reduced variability after wearing the *SEAExo* with assistance, indicating a beneficial effect on gait stability and consistency. In particular, five participants with obvious gait asymmetry ratio (i.e., $R_{SI} > 15\%$, $R_{SI} = |1 - SI| \times 100\%$) significantly ($t(8) = 4.01$, $p < 0.05$, see subplot of **Fig. 4G**) benefited from the active robotic assistance to improve their temporal gait symmetry (i.e., R_{SI} of P1, P2, P3, P5, and P6 were reduced by 48.1%, 57.7%, 38.1%, 50.1%, and 82.9%, respectively) compared to the baseline. Significant reduction in the swing duration asymmetry ratio was also found in the same participant group ($t(8) = 3.41$, $p < 0.05$, see subplot of **Fig. 4I**). Furthermore, those participants with severe gait asymmetry (i.e., P1, P2, and P3, $R_{SI} > 30\%$) were also assisted by torques with larger amplitudes. According to [31], there was a normative *SI* range of 10%. A participant whose gait symmetry was near this range (i.e., P4 and P7) had smaller changes in gait symmetry indices in *Passive* and *Hybrid* sessions. Interestingly, P2 showed a dramatic symmetry increase by 39.1% in the *Passive* session.

C. Effects on the Muscular Activities

The *SEAExo* statistically influenced participats' muscle activities of LG and MG muscles on the paretic side in group level (LG: $F(2,5) = 28.98$, $p < 0.05$, MG: $\chi^2(2) = 10.57$, $p < 0.05$). The presented net changes in muscular activities were calculated as a percentage of the median MAVs in the baseline, i.e., $(MAV_{hybrid} - MAV_{NoExo})/MAV_{NoExo} \times 100\%$. Seeing **Fig. 4J**, the muscle activities of LG and MG muscles significantly reduced by 27.9% ($t(12) = 4.08$, $p < 0.05$) and 38.5% ($Z = 2.67$, $p < 0.05$) in *Passive* session, and 22.8% ($t(12) = 3.04$, $p < 0.05$) and 51.3% ($Z = 2.94$, $p < 0.05$) in *Hybrid* session. In the individual level, both the *Passive* and *Hybrid* conditions showed adverse effects on the muscle activities of knee extensors in P1, P3, and P7.

IV. DISCUSSION

This study was built on prior clinical, biomechanical, and usability evaluations of a unilateral exoskeleton *SEAExo* in people with subacute stroke. All participants completed trials for all sessions without any uncomfortable feedback. *SEAExo* could be adjusted to fit a wide range of body sizes successfully. The exoskeleton structure served as a knee-ankle-foot orthosis mitigating knee hyperextension during the mid-stance and ankle inversion/eversion throughout the swing phase. When the *SEAExo* worked in F.T.C mode, the assistance profile could be manually tuned to adjust to the user's gait pattern and achieve a user preferred assistance. Combing with the elastic bands, *SEAExo* could provide whole-leg assistance during a gait cycle. The controller was designed to generate assistance based on the gait characteristics of the non-paretic side.

A. Assistance Magnitude and Peak Timing

Unsurprisingly, the personalized assistance profiles differed dramatically across participants due to their varied physical conditions, e.g., heterogeneous pathological gait patterns, muscle spasticity levels, and body sizes. Besides, it turned out that the assistance amplitude P_i and peak timing $\overline{\alpha_i}$ had a significant impact on gait metrics improvements, consistent with [32]. The rising/falling slope values k_i did not present a significant difference (see **Table II**). Regarding the assistance's amplitudes, we applied relatively smaller magnitudes

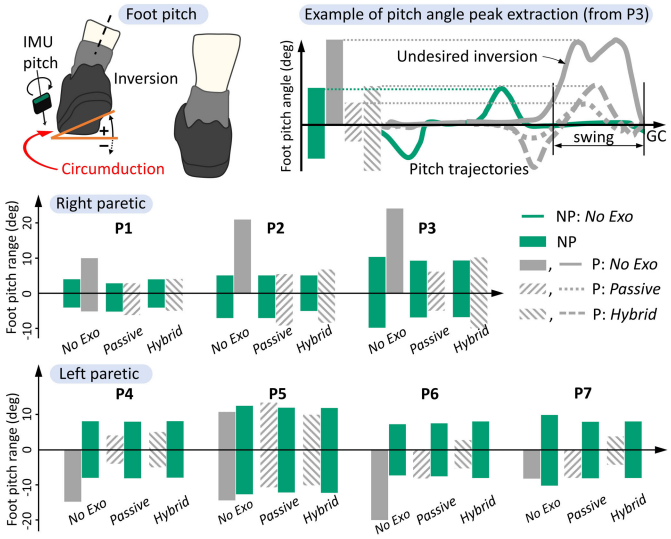

Fig. 5. Illustration of foot pitch angle (measured via instep-mounted IMU) and foot pitch peak symmetry. X-axis denotes the sagittal plane. Pitch angle offsets of IMU due to mounting have been eliminated.

than the single-joint exoskeletons, e.g., the unilateral soft ankle exoskeleton [25] and knee exoskeleton [26]. The reasons might explain this: 1). The *SEAExo* assisted the whole paretic leg, contributing to more considerable net benefits. During the multi-joint assistance, participants' subconscious walking strategy could maximize the overall benefits from the whole-leg assistance resulting in smaller magnitudes than the single-joint assistance, consistent with the human-in-the-loop optimized results in [21]; 2). the *SEAExo* unilaterally assisted the user's paretic leg. Large assistance amplitude might lead to an unbalanced walking pattern and decrease user's acceptance at the early stage of robot-aided gait training. Significantly, the assistance magnitude should be diminished if the joint spasticity of the paretic leg decreased and the propulsion symmetry of both sides was reduced (translated into a higher Brunnstrom stage). This explained that the participants with moderate spasticity (i.e., P4, P5, P6, and P7; Brunnstrom stage IV or V) preferred mild assistance, and participants with more significant muscle spasticity (i.e., P1, P2, and P3, Brunnstrom stage III) were able to adapt to larger assistance magnitudes.

As shown in **Fig. 4F**, participants' median stance duration percentage values can be translated into TO timings when normalized to the gait cycle starting from IC. Hence, we can transfer the results of personalized assistance's peak timings into: the *PF* assistance peaked at 49.2[36.3, 62.0] %GC; the *DF* assistance peaked at 86.4[77.5, 97.5] %GC; and the *KF* assistance peaked at 75.1[60.5, 94.9] %GC. Based on the reported joint kinetics from a group of stroke survivors [33], the average *KF* torques peaked at 60-65 %GC, and the *PF* and *DF* torques peaked at 45-50 %GC and 5-10 %GC, respectively (see **Fig. 4A&B**). Therefore, a user preferred assistance was not simply a mimic of the biological toque profile. The peak timings of the user preferred *KF* and *PF* assistance partially overlapped with biological joint torques. While the peak timings of *DF* torques were all earlier than biological torques due to foot-drop. In addition, we also found that the increase of muscle spasticity resulted in later *KF* assistance peaks and peaks of *DF* assistance that were closer to biological ones (see P1, P2, and P3). In contrast, the optimized results in [21] revealed that torques peaked later than the biological peaks of the knee and ankle joints contributed to more metabolic cost reduction in non-disabled people, indicating that different research goals and different walking adaption strategies to robotic assistance between healthy people and stroke survivors led to varied parameter settings. These findings would inform the presetting and tuning of exoskeletons' assistance parameters for post-stroke gait rehabilitation.

B. Biomechanical Outcomes

Compared to the other two sessions, we can see a consistent tendency in the *Hybrid* session that participants exhibited healthier gait kinematics with foot contact angle and knee flexion peak closer to the normal level (dashed lines in **Fig. 4D&E**) and more symmetric gait pattern, signifying better inter-limb movements symmetry. Interestingly, improvements, i.e., the increased foot contact angle on the unassisted ankle joint and dramatically enhanced gait symmetry of P2, were also found in *Passive* session. Moreover, for the participants who exhibited moderate gait asymmetry in *No Exo* session (i.e., P4 and P7), personalized assistance not only improved their joint kinematics (specifically an increase in the ankle contact angle by 4.6° and 7.2° and an increase in knee flexion angle by 24.0° and 9.3°) but also had a minimal impact on their temporal gait symmetry. These findings demonstrated that stroke survivors would adjust their kinematic and kinetic adaption strategies to maximize the benefit got from *SEAExo* with or without active assistance. It was also reported that an average of 109 min. of training time contributed to better assistive performance [34], and participants can tolerate higher assistance amplitude with increased training time [20]. These results bring us confidence in applying *SEAExo* in post-stroke gait rehabilitation with a longer training time and a higher assistance magnitude (the maximum assistance applied in this study was less than 30% of the system's output capacity).

Moreover, we established another kinematic index, i.e., the foot pitch angle. The foot pitch angle bias of the paretic foot is caused by compound effects of ankle inversion/eversion and circumduction [35]. A healthy gait pattern exhibits a symmetric foot pitch relative to the sagittal plane (see **Fig. 5**). Ankle eversion/inversion during swing phase (translated into extreme pitch angle) was most undesirable, which increased the risk of falling. It can be seen from the results in *Passive* session that the exoskeleton's rigid frame resulted in reduced foot pitch deviations, and the remaining foot pitch deviations might be related to residual circumduction that was not eliminated. Then, the foot pitch biases were further reduced and more symmetric about the sagittal plane with the active exoskeleton assistance, demonstrating the effectiveness of the proposed control strategy on the mitigation of deficits and compensatory movement (i.e., ankle inversion/eversion and circumduction).

Reductions in muscle activities were obtained in the muscles that acted in the exact directions as exoskeleton assistance (i.e., TA, LG, MG, and HM). At the same time, changes in the activities of knee extensors varied across participants. Typically, P1, P3, and P7 showed increased muscle activities

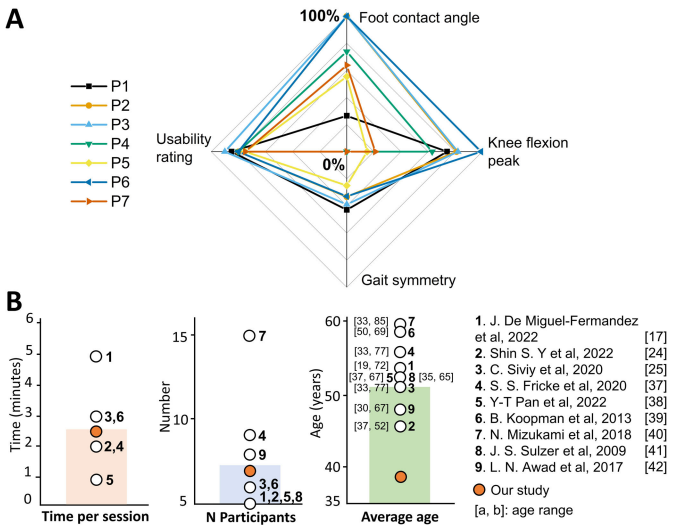

Fig. 6. **A**. Overall benefits of interest (*Hybrid* v.s *No Exo*). The improvement percentages of foot contact angle that over 100% were set to 100% for better presentation (i.e., P2, P3, and P6). Gait symmetry change percentage equals to zero means no obvious improvement (i.e., P4 and P7). **B**. Comparison with relevant studies in terms of the duration of each session and the number/average age of participants.

in both the *Passive* and *Hybrid* sessions. Muscle activities decreased in the *Passive* session might be associated with the compensatory strategy and complex leg dynamics during walking. Because of the stiff knee and foot drop, stroke survivors usually adopt hip hiking to achieve energy-efficient stepping with less knee and ankle movements [36]. With passive assistance from elastic bands, the participants can complete the hip flexion more easily, which further reduced the muscle activities of knee and ankle joints. From this point of view, *SEAExo* in *Passive* condition tended to aggravate the hip hiking due to the passive assistance and added weight on the paretic limb, and it worked positively only when its contribution to concentric contraction was greater than the energy cost of hip extension. Hence, the increase of muscle activities participants (P1, P3, and P7) probably indicated that the bands' stiffness were insufficient and suggested a customized approach in the future setup. Besides, it was reported that increased knee flexion in the swing phase could relieve hip hiking during walking [36], signifying the necessity of active assistance on the knee joint.

In this section, we also found that a single biomechanical metric did not necessarily imply a healthy gait (combing the results presented in **Fig. 4&5**). This finding informs the studies focused on the optimization strategies that strategies with single biomechanical metric (e.g., temporal gait symmetry) may not be robust for post-stroke gait rehabilitation. Appropriate biomechanical objectives should be measured and evaluated to modulate robotic assistance to achieve enhanced efficacy.

C. Usability and Limitations

The overall usability score was 8.1 ± 0.5 points, demonstrating users' satisfaction with the device and applied control strategy. The low-profile and lightweight characteristics of *SEAExo* ensured its wearability. It improved the users' joint kinematics and gait symmetry and helped users to walk with less effort. Nevertheless, lower scores were given by P5 and P7 because they only perceived the changes in muscle activities due to their moderate deficits, which suggested that we should establish appropriate expectations for participants before the robot-aided gait rehabilitation to achieve user's satisfaction and acceptance. Finally, the overall benefits for all participants are presented in **Fig. 6A**.

However, this study was subject to several limitations. First, the exposure time for the participants was limited due to their ongoing therapies at the time of study enrollment. The results, while positive, were sub-optimal on account of insufficient user training time with *SEAExo*. The assistive performance of *SEAExo* with a longer training time and a higher assistance magnitude should be investigated in future work. Besides, the small sample size of this study ($n = 7$) could lead to less power of statistics. In comparison, the same limitation can be found in similar clinical research for people with stroke (7.1 ± 3.1 participants were recruited in [17], [24], [25], [37], [38], [39], [40], [41] and [42], see **Fig. 6B**). However, the average age of recruited participants is younger than that (53.2 ± 13.8 years) in these studies, limiting the extension of this study's findings to the elderly stroke population. Lastly, a treadmill-based experiment did not allow us to observe the impacts on walking speed changes, which is also an effective predictor for gait performance.

V. Conclusion

In conclusion, this study presented a newly designed exoskeleton that was satisfied by participants after stroke. The positive biomechanical outcomes demonstrate that *SEAExo* with personalized assistance can instantly improve the gait biomechanics of people post-stroke. We found increased foot contact angle and knee flexion peak, reduced muscle activities on the paretic side. Enhanced gait symmetry were observed in more impaired participants. In addition, we found consistency in user-preferred assistance timing parameters, which could provide insights for parameter tuning of exoskeleton assistance based on gait events or joint kinetics. User preference can significantly reduce the time consumption of the tuning process, and the role of the elastic bands is mainly reflected in reducing muscle activities of knee extensors and assisting hip flexion motion. These findings illustrate the efficacy of *SEAExo* for clinical gait rehabilitation. Future studies will focus on the research that evaluates the maximum efficacy of *SEAExo* on post-stroke gait rehabilitation with a larger sample size and longer training time. We will also investigate how people post-stroke adapt to exoskeleton assistance with long-term training.

Acknowledgment

The authors express thanks to Qiyin Huang (Ph.D. candidate with the University of Minnesota) in helping with data analysis.

References

[1] V. L. Feigin et al., "World Stroke Organization (WSO): Global stroke fact sheet 2022," *Int. J. Stroke*, vol. 17, no. 1, pp. 18–29, Jan. 2022.

[2] K. J. Nolan et al., "Utilization of robotic exoskeleton for overground walking in acute and chronic stroke," *Frontiers Neurorobotics*, vol. 15, Sep. 2021, Art. no. 689363.

[3] J. J. Eng and P.-F. Tang, "Gait training strategies to optimize walking ability in people with stroke: A synthesis of the evidence," *Exp. Rev. Neurotherapeutics*, vol. 7, no. 10, pp. 1417–1436, Oct. 2007.

[4] B. French et al., "Does repetitive task training improve functional activity after stroke? A Cochrane systematic review and meta-analysis," *J. Rehabil. Med., Off. J. Uems Eur. Board Phys. Rehabil. Med.*, vol. 42, no. 1, pp. 9–14, 2010.

[5] A. Rodríguez-Fernández, J. Lobo-Prat, and J. M. Font-Llagunes, "Systematic review on wearable lower-limb exoskeletons for gait training in neuromuscular impairments," *J. NeuroEng. Rehabil.*, vol. 18, no. 1, pp. 1–21, Dec. 2021.

[6] H. K. Kwa, J. H. Noorden, M. Missel, T. Craig, J. E. Pratt, and P. D. Neuhaus, "Development of the IHMC mobility assist exoskeleton," in *Proc. IEEE Int. Conf. Robot. Autom.*, May 2009, pp. 2556–2562.

[7] L. Yeung et al., "Design of an exoskeleton ankle robot for robot-assisted gait training of stroke patients," in *Proc. Int. Conf. Rehabil. Robot. (ICORR)*, Jul. 2017, pp. 211–215.

[8] T. Xue, Z. Wang, T. Zhang, and M. Zhang, "Adaptive oscillator-based robust control for flexible hip assistive exoskeleton," *IEEE Robot. Autom. Lett.*, vol. 4, no. 4, pp. 3318–3323, Oct. 2019.

[9] T. Lenzi, M. C. Carrozza, and S. K. Agrawal, "Powered hip exoskeletons can reduce the user's hip and ankle muscle activations during walking," *IEEE Trans. Neural Syst. Rehabil. Eng.*, vol. 21, no. 6, pp. 938–948, Nov. 2013.

[10] A. Martínez, B. Lawson, and M. Goldfarb, "A controller for guiding leg movement during overground walking with a lower limb exoskeleton," *IEEE Trans. Robot.*, vol. 34, no. 1, pp. 183–193, Feb. 2018.

[11] T. Yan et al., "A novel adaptive oscillators-based control for a powered multi-joint lower-limb orthosis," in *Proc. IEEE Int. Conf. Rehabil. Robot. (ICORR)*, Aug. 2015, pp. 386–391.

[12] Y. Fang, G. Orekhov, and Z. F. Lerner, "Improving the energy cost of incline walking and stair ascent with ankle exoskeleton assistance in cerebral palsy," *IEEE Trans. Biomed. Eng.*, vol. 69, no. 7, pp. 2143–2152, Jul. 2022.

[13] J. R. Koller, D. A. Jacobs, D. P. Ferris, and C. D. Remy, "Learning to walk with an adaptive gain proportional myoelectric controller for a robotic ankle exoskeleton," *J. NeuroEng. Rehabil.*, vol. 12, no. 1, pp. 1–14, Dec. 2015.

[14] J. Zhang et al., "Human-in-the-loop optimization of exoskeleton assistance during walking," *Science*, vol. 356, no. 6344, pp. 1280–1284, Jun. 2017.

[15] Y. Ding, M. Kim, S. Kuindersma, and C. J. Walsh, "Human-in-the-loop optimization of hip assistance with a soft exosuit during walking," *Sci. Robot.*, vol. 3, no. 15, Feb. 2018, Art. no. eaar5438.

[16] S. Song and S. H. Collins, "Optimizing exoskeleton assistance for faster self-selected walking," *IEEE Trans. Neural Syst. Rehabil. Eng.*, vol. 29, pp. 786–795, 2021.

[17] J. de Miguel-Fernández et al., "Immediate biomechanical effects of providing adaptive assistance with an ankle exoskeleton in individuals after stroke," *IEEE Robot. Autom. Lett.*, vol. 7, no. 3, pp. 7574–7580, Jul. 2022.

[18] R. L. Medrano, G. C. Thomas, and E. J. Rouse, "Can humans perceive the metabolic benefit provided by augmentative exoskeletons?" *J. NeuroEng. Rehabil.*, vol. 19, no. 1, pp. 1–13, Dec. 2022.

[19] B. Zhong, W. Niu, E. Broadbent, A. McDaid, T. M. C. Lee, and M. Zhang, "Bringing psychological strategies to robot-assisted physiotherapy for enhanced treatment efficacy," *Frontiers Neurosci.*, vol. 13, p. 984, Sep. 2019.

[20] K. A. Ingraham, C. D. Remy, and E. J. Rouse, "The role of user preference in the customized control of robotic exoskeletons," *Sci. Robot.*, vol. 7, no. 64, Mar. 2022.

[21] P. W. Franks, G. M. Bryan, R. M. Martin, R. Reyes, A. C. Lakmazaheri, and S. H. Collins, "Comparing optimized exoskeleton assistance of the hip, knee, and ankle in single and multi-joint configurations," *Wearable Technol.*, vol. 2, p. e16, Jan. 2021.

[22] S.-H. Lee et al., "Wearable hip-assist robot modulates cortical activation during gait in stroke patients: A functional near-infrared spectroscopy study," *J. NeuroEng. Rehabil.*, vol. 17, no. 1, pp. 1–8, Dec. 2020.

[23] Y. Qian, S. Han, Y. Wang, H. Yu, and C. Fu, "Toward improving actuation transparency and safety of a hip exoskeleton with a novel nonlinear series elastic actuator," *IEEE/ASME Trans. Mechatronics*, vol. 28, no. 1, pp. 417–428, Feb. 2023.

[24] S. Y. Shin, K. Hohl, M. Giffhorn, L. N. Awad, C. J. Walsh, and A. Jayaraman, "Soft robotic exosuit augmented high intensity gait training on stroke survivors: A pilot study," *J. NeuroEng. Rehabil.*, vol. 19, no. 1, pp. 1–12, Jun. 2022.

[25] C. Siviy et al., "Offline assistance optimization of a soft exosuit for augmenting ankle power of stroke survivors during walking," *IEEE Robot. Autom. Lett.*, vol. 5, no. 2, pp. 828–835, Apr. 2020.

[26] A. C. Villa-Parra et al., "Control of a robotic knee exoskeleton for assistance and rehabilitation based on motion intention from sEMG," *Res. Biomed. Eng.*, vol. 34, no. 3, pp. 198–210, Jul. 2018.

[27] J. S. Lora-Millan, F. J. Sanchez-Cuesta, J. P. Romero, J. C. Moreno, and E. Rocon, "A unilateral robotic knee exoskeleton to assess the role of natural gait assistance in hemiparetic patients," *J. NeuroEng. Rehabil.*, vol. 19, no. 1, pp. 1–24, Oct. 2022.

[28] B. Zhong, K. Guo, H. Yu, and M. Zhang, "Toward gait symmetry enhancement via a cable-driven exoskeleton powered by series elastic actuators," *IEEE Robot. Autom. Lett.*, vol. 7, no. 2, pp. 786–793, Apr. 2022.

[29] A.-L. Hsu, P.-F. Tang, and M.-H. Jan, "Analysis of impairments influencing gait velocity and asymmetry of hemiplegic patients after mild to moderate stroke," *Arch. Phys. Med. Rehabil.*, vol. 84, no. 8, pp. 1185–1193, Aug. 2003.

[30] G. Bovi, M. Rabuffetti, P. Mazzoleni, and M. Ferrarin, "A multiple-task gait analysis approach: Kinematic, kinetic and EMG reference data for healthy young and adult subjects," *Gait Posture*, vol. 33, no. 1, pp. 6–13, Jan. 2011.

[31] M. Plotnik, J. M. Wagner, G. Adusumilli, A. Gottlieb, and R. T. Naismith, "Gait asymmetry, and bilateral coordination of gait during a six-minute walk test in persons with multiple sclerosis," *Sci. Rep.*, vol. 10, no. 1, pp. 1–11, Jul. 2020.

[32] J. de Miguel-Fernandez et al., "Relationship between ankle assistive torque and biomechanical gait metrics in individuals after stroke," *TechRxiv*, 2022, doi: 10.36227/techrxiv.20749789.v1.

[33] N. D. Neckel, N. Blonien, D. Nichols, and J. Hidler, "Abnormal joint torque patterns exhibited by chronic stroke subjects while walking with a prescribed physiological gait pattern," *J. NeuroEng. Rehabil.*, vol. 5, no. 1, pp. 1–13, Dec. 2008.

[34] K. L. Poggensee and S. H. Collins, "How adaptation, training, and customization contribute to benefits from exoskeleton assistance," *Sci. Robot.*, vol. 6, no. 58, Sep. 2021, Art. no. eabf1078.

[35] T. Seel, C. Werner, and T. Schauer, "The adaptive drop foot stimulator—Multivariable learning control of foot pitch and roll motion in paretic gait," *Med. Eng. Phys.*, vol. 38, no. 11, pp. 1205–1213, Nov. 2016.

[36] T. Akbas, S. Prajapati, D. Ziemnicki, P. Tamma, S. Gross, and J. Sulzer, "Hip circumduction is not a compensation for reduced knee flexion angle during gait," *J. Biomechanics*, vol. 87, pp. 150–156, Apr. 2019.

[37] S. S. Fricke, H. J. G. Smits, C. Bayón, J. H. Buurke, H. Van Der Kooij, and E. H. F. van Asseldonk, "Effects of selectively assisting impaired subtasks of walking in chronic stroke survivors," *J. NeuroEng. Rehabil.*, vol. 17, no. 1, pp. 1–13, Dec. 2020.

[38] Y.-T. Pan et al., "Effects of bilateral assistance for hemiparetic gait post-stroke using a powered hip exoskeleton," *Ann. Biomed. Eng.*, vol. 51, pp. 410–421, Feb. 2022.

[39] B. Koopman, E. H. Van Asseldonk, and H. Van Der Kooij, "Selective control of gait subtasks in robotic gait training: Foot clearance support in stroke survivors with a powered exoskeleton," *J. neuroeng. Rehabil.*, vol. 10, no. 1, pp. 1–21, 2013.

[40] N. Mizukami et al., "Effect of the synchronization-based control of a wearable robot having a non-exoskeletal structure on the hemiplegic gait of stroke patients," *IEEE Trans. Neural Syst. Rehabil. Eng.*, vol. 26, no. 5, pp. 1011–1016, May 2018.

[41] J. S. Sulzer, R. A. Roiz, M. A. Peshkin, and J. L. Patton, "A highly backdrivable, lightweight knee actuator for investigating gait in stroke," *IEEE Trans. Robot.*, vol. 25, no. 3, pp. 539–548, Jun. 2009.

[42] L. N. Awad et al., "Reducing circumduction and hip hiking during hemiparetic walking through targeted assistance of the paretic limb using a soft robotic exosuit," *Amer. J. Phys. Med. Rehabil.*, vol. 96, no. 10, pp. S157–S164, 2017.